

## ON SOLUTIONS OF SACHERER INTEGRAL EQUATION

S. Y. Zhang

October 1993

Collider Accelerator Department  
**Brookhaven National Laboratory**

**U.S. Department of Energy**

USDOE Office of Science (SC)

Notice: This technical note has been authored by employees of Brookhaven Science Associates, LLC under Contract No.DE-AC02-76CH00016 with the U.S. Department of Energy. The publisher by accepting the technical note for publication acknowledges that the United States Government retains a non-exclusive, paid-up, irrevocable, world-wide license to publish or reproduce the published form of this technical note, or allow others to do so, for United States Government purposes.

## **DISCLAIMER**

This report was prepared as an account of work sponsored by an agency of the United States Government. Neither the United States Government nor any agency thereof, nor any of their employees, nor any of their contractors, subcontractors, or their employees, makes any warranty, express or implied, or assumes any legal liability or responsibility for the accuracy, completeness, or any third party's use or the results of such use of any information, apparatus, product, or process disclosed, or represents that its use would not infringe privately owned rights. Reference herein to any specific commercial product, process, or service by trade name, trademark, manufacturer, or otherwise, does not necessarily constitute or imply its endorsement, recommendation, or favoring by the United States Government or any agency thereof or its contractors or subcontractors. The views and opinions of authors expressed herein do not necessarily state or reflect those of the United States Government or any agency thereof.

Accelerator Division  
Alternating Gradient Synchrotron Department  
BROOKHAVEN NATIONAL LABORATORY  
Upton, New York 11973

Accelerator Division  
Technical Note

**AGS/AD/Tech. Note No. 381**

**ON SOLUTIONS OF SACHERER INTEGRAL EQUATION**

S.Y. Zhang and W.T. Weng

October 12, 1993

# ON SOLUTIONS OF SACHERER INTEGRAL EQUATION \*

*S.Y. Zhang and W.T. Weng*

AGS Department, Brookhaven National Laboratory,  
Upton, New York 11973

## ABSTRACT

There are basically two approaches in solving the Sacherer integral equation, one uses the orthogonal polynomial expansion for radial functions, and another uses the Hankel harmonic samplings, both have extensive application. In this article, we discuss these approaches and present the corresponding solutions. If the azimuthal modes are not coupled, the Sacherer integral equation can be treated as an eigenvalue problem. It is shown that the information provided by the eigenvalue alone are insufficient in determining the system response. The initial perturbation pattern with respect to the radial modes must be considered. Several particle distributions are used as examples to show the solutions to the equation, and the physical implication of the radial modes is illustrated by using the examples.

---

\* Work performed under the auspices of the U.S. Department of Energy

## I. Introduction

The coherent bunched beam instability can be described by the Sacherer integral equation [1], developed from the Vlasov equation on the particle evolution in phase space given impedances from the environment. The Sacherer integral equation (SIE) nowadays also becomes a foundation for further analysis of complicated beam dynamics, such as the microwave instability, the bunch lengthening, and various kinds of mode couplings [2,3].

If the azimuthal modes are not coupled, such as in a low intensity regime, then the SIE can be reduced to an eigenvalue problem, where the two unknown variables, i.e. the coherent frequency shift and the radial function can be solved separately. There are basically two approaches in solving the SIE, and both have extensive applications. One is using the orthogonal polynomial expansion for radial functions [4,5], and another is using Hankel harmonic samplings for radial functions [3].

The approach using orthogonal polynomials is conventional in treating problems such as the Sacherer integral equation. By using the lowest  $\bar{k}$  orthogonal polynomials for the radial mode expansion, the SIE is transformed into a  $\bar{k}$ th order linear system. To determine the stability of the system, usually the eigenvalues should be found. However, in determining the system response, the information of eigenvalues alone is insufficient, the initial perturbation with respect to the radial modes must be included. In an extreme case, some eigenvalues, including unstable ones, may be virtually ineffective, in coupling to the initial perturbation.

In this article, we study the solutions for the Sacherer integral equation. We start from the orthogonal polynomial approach, and concentrate on the issues related to the radial modes. Using only necessary analytic mathematical means, the equation will be solved for several particle distributions, and the physical implications related to the radial modes are presented. The approach using Hankel harmonic samplings is also studied, and the relation and comparison of the two approaches are discussed.

axis,

$$\lambda(\phi) = \int_{-\infty}^{\infty} \psi_p(\phi, \dot{\phi}/\omega_S) d\dot{\phi}/\omega_S \quad (2-9)$$

The line density can be Fourier expanded as,

$$\lambda(\phi) = \frac{1}{2\pi} \sum_{p=-\infty}^{\infty} \Lambda(p) e^{jp\phi} \quad (2-10)$$

where the spectrum is,

$$\Lambda(p) = \int_{-\infty}^{\infty} \lambda(\phi) e^{-jp\phi} d\phi \quad (2-11)$$

Note that in the transform the variable is the phase deviation  $\phi$ , rather than the conventional time  $t$ . Using (2-10), we obtain,

$$V_p(\phi) = -I_0 e^{j\omega t} \sum_{p=-\infty}^{\infty} Z(p) \Lambda(p) e^{jp\phi} \quad (2-12)$$

where  $I_0$  is the beam average current and  $Z(p)$  is the impedance corresponding to the spectrum  $\Lambda(p)$ . Substituting (2-12) into (2-8), we get,

$$\ddot{\phi} + \omega_S^2 \phi = - \frac{\omega_S^2 I_0}{V \cos \phi_S} e^{j\omega t} \sum_{p=-\infty}^{\infty} Z(p) \Lambda(p) e^{jp\phi} \quad (2-13)$$

We emphasize that  $V_p(\phi)$  is the voltage generated by the line density  $\lambda(\phi)$  in (2-9), which applies only to the particles with the phase position  $\phi$ .

The perturbation distribution can be written,

$$\psi_p(r, \theta) = \sum_{m'=-\infty}^{\infty} R^{(m')}(r) e^{jm'\theta} \quad (2-14)$$

where  $R^{(m')}(r)$  is the radial function with the  $m'$ th azimuthal mode. Substituting (2-13), (2-14) into (2-7), and leaving off  $e^{j\omega t}$ , we get,

$$j \sum_{m'=-\infty}^{\infty} (\omega - m' \omega_S) R^{(m')}(r) e^{jm'\theta} = \frac{\omega_S I_0}{V \cos \phi_S} \sin \theta \frac{d\psi_0}{dr} \sum_{p=-\infty}^{\infty} Z(p) \Lambda(p) e^{jp\phi} \quad (2-15)$$

Multiplying both sides of (2-15) by  $e^{-jm'\theta}$ , and integrating over  $\theta$  from 0 to  $2\pi$ , we get,

$$(\omega - m \omega_S) R^{(m)}(r) = j^{m+1} \frac{m \omega_S I_0}{V \cos \phi_S} \frac{d\psi_0}{dr} \frac{1}{r} \sum_{p=-\infty}^{\infty} \frac{Z(p)}{p} J_m(pr) \Lambda(p) \quad (2-16)$$

$$W(r) = \frac{d\psi_0}{dr} \frac{1}{r} \quad (2-24)$$

and also,

$$\xi = \frac{2\pi I_0}{V \cos \phi_S} \quad (2-25)$$

### III. Solution Using Orthogonal Polynomials

#### 3.1. Eigenvalue Problem

If the azimuthal modes are not coupled, then only the force generated by the radial function  $R^{(m)}(r)$  is responsible to the coherent motion  $\omega$  in (2-23), the original Sacherer integral equation (2-16) is simplified as,

$$(\omega - m\omega_S)R^{(m)}(r) = jm\omega_S\xi W(r) \sum_{p=-\infty}^{\infty} \frac{Z(p)}{p} J_m(pr) \int_0^{\infty} R^{(m)}(r') J_m(pr') r' dr' \quad (3-1)$$

Thus, the SIE can be transformed to an eigenvalue problem, which is eligible to solve separately for two unknown variables, i.e., the coherent frequency  $\omega$  and the radial function  $R^{(m)}(r)$ .

For the weight function  $W(r)$ , a set of normalized orthogonal polynomials  $f_k(r)$  can always be found such that,

$$\int_0^{\infty} W(r) f_k(r) f_l(r) r dr = \delta_{k,l} \quad (3-2)$$

Using the orthogonal polynomial, the radial function can be written as,

$$R^{(m)}(r) = W(r) \sum_{k'=0}^{\infty} \alpha_{k'}^{(m)} f_{k'}(r) \quad (3-3)$$

Define the Hankel spectrum for the orthogonal polynomial,

$$\Lambda_k^{(m)}(p) = \int_0^{\infty} W(r) f_k(r) J_m(pr) r dr \quad (3-4)$$

Then we have

$$\Lambda^{(m)}(p) = \sum_{k'=0}^{\infty} \alpha_{k'}^{(m)} \Lambda_{k'}^{(m)}(p) \quad (3-5)$$

which is an eigenvalue problem. The eigenvalues can be solved through the equation

$$| \lambda \mathbf{I} - jm \omega_s \xi \mathbf{M} | = 0 \quad (3-12)$$

where  $\mathbf{I}$  is identity matrix, and

$$\lambda = \omega - m \omega_s \quad (3-13)$$

We note that the eigenvector

$$\alpha^{(m)} = \begin{bmatrix} \alpha_1^{(m)} \\ \cdot \\ \cdot \\ \alpha_{\bar{k}}^{(m)} \end{bmatrix} \quad (3-14)$$

is not presented in (3-12) and therefore it will not directly affect the solution of the coherent frequency.

### 3.2. Radial Modes

Using the expansion of the radial function  $R^{(m)}(r)$  by the orthogonal functions, as shown in (3-3), the Sacherer integral equation (3-1) has been transformed to a linear system (3-11) with an order  $\bar{k}$ . We have assumed that the higher order modes are not important with respect to the system response.

Define

$$\mathbf{Z} = \text{diag} \left\{ \frac{Z(p)}{p} \right\} = \begin{bmatrix} \frac{Z(-\bar{p})}{-\bar{p}} & 0 & \dots & 0 \\ 0 & \frac{Z(-\bar{p}+1)}{-\bar{p}+1} & \cdot & 0 \\ \cdot & \cdot & \cdot & \cdot \\ 0 & 0 & \dots & \frac{Z(\bar{p})}{\bar{p}} \end{bmatrix} \quad (3-15)$$

and

$$\Lambda = \begin{bmatrix} \Lambda_1^{(m)}(-\bar{p}) & \dots & \Lambda_1^{(m)}(\bar{p}) \\ \cdot & \cdot & \cdot \\ \Lambda_{\bar{k}}^{(m)}(-\bar{p}) & \dots & \Lambda_{\bar{k}}^{(m)}(\bar{p}) \end{bmatrix} \quad (3-16)$$

where

$$\alpha_{(i)}^{(m)} = \begin{bmatrix} \alpha_{(i),1}^{(m)} \\ \cdot \\ \alpha_{(i),\bar{k}}^{(m)} \end{bmatrix} \quad (3-23)$$

The corresponding radial function

$$R_{(i)}^{(m)}(r) = W(r) \sum_{k'=0}^{\infty} \alpha_{(i),k'}^{(m)} f_{k'}(r) \quad (3-24)$$

is the  $i$ th radial mode. Substituting the  $i$ th eigenvalue  $\lambda_{(i)}$  and the corresponding radial mode  $R_{(i)}^{(m)}(r)$  into (3-1), the Sacherer integral equation is satisfied. This indicates that according to the SIE if the perturbation distribution is dominated by the  $i$ th radial mode, i.e.

$$\psi_p(r, \theta) = R_{(i)}^{(m)}(r) e^{jm\theta} \quad (3-25)$$

then only the coherent frequency shift  $\lambda_{(i)}$  is excited, and other eigenvalues are virtually not presented.

To show the complication implied by the existence of  $\bar{k}$  eigenvalues and also  $\bar{k}$  associated eigenvectors, the following elaborations are needed. We rewrite the equation (3-11) as,

$$\lambda \alpha = \mathbf{M}_1 \alpha \quad (3-26)$$

Taking Laplace transform, we have

$$s \alpha(s) - \alpha_0 = \mathbf{M}_1 \alpha(s) \quad (3-27)$$

where  $\alpha_0$  is the initial condition of the vector  $\alpha$  in time domain, i.e.  $\alpha_0 = \alpha(0_-)$ . Since the orthogonal polynomials have been chosen, this can be interpreted as the initial perturbation distribution with respect to the radial modes, as shown in (2-14) and (3-3). Using partial fraction expansion, the evolution of the perturbation can be described as,

$$\alpha(s) = (s\mathbf{I} - \mathbf{M}_1)^{-1} \alpha_0 = \sum_{i=1}^{\bar{k}} \frac{\mathbf{t}_{(i)} \bar{\mathbf{t}}_{(i)}}{s - \lambda_{(i)}} \alpha_0 \quad (3-28)$$

where  $\bar{\mathbf{t}}_{(i)}$  is the  $i$ th row of the matrix  $\mathbf{T}^{-1}$ , and the relation used in the second step can be

through for most cases. For instance, if two eigenvalues are the same as  $\lambda_{(i)}$ , instead of one with  $\lambda_{(i)}$  and another with  $\lambda_{(k)}$ , then the second mode will be  $t e^{j\lambda_{(i)}t}$  instead of  $e^{j\lambda_{(k)}t}$ .

#### IV. Examples for Several Distributions

In this section, we present solution of the Sacherer integral equation for several particle distributions by using the orthogonal polynomial approach. For each distribution, the corresponding orthogonal polynomials are found [6]. The remaining calculation are performed numerically by using the equations shown in the last section. Some closed forms for the Hankel spectra can be found in [7]. The physical implication of the radial modes will be discussed. For convenience, these discussion will be placed in the section of the Gaussian distribution.

##### 4.1. Gaussian Distribution

For a Gaussian distribution, the stationary phase space density is

$$\psi_0(r) = \frac{2}{\pi \hat{r}^2} e^{-2r^2/\hat{r}^2} \quad (4-1)$$

where  $\hat{r}$  is the effective half bunch length in phase space. The line density is also a Gaussian,

$$\lambda_0(\phi) = \frac{\sqrt{2}}{\sqrt{\pi}} \frac{1}{\phi} e^{-2\phi^2/\hat{\phi}^2} \quad (4-2)$$

where  $\hat{\phi}$  is the effective half bunch length in phase deviation, which is in fact equal to  $\hat{r}$ . For Gaussian distribution, we have

$$\hat{\phi} = 2\sigma \quad (4-3)$$

where  $\sigma$  is the standard deviation of Gaussian distribution.

The weight function can be calculated as

$$W(r) = \frac{-8}{\pi \hat{r}^4} e^{-2r^2/\hat{r}^2} \quad (4-4)$$

First, we find a set of orthogonal polynomials according to the weight function. The

obtained by,

$$\lambda_{(i)}^{(m)}(\phi) = \frac{j^m}{2\pi} \sum_{p=-\infty}^{\infty} \Lambda_{(i)}^{(m)}(p) e^{jp\phi} = \frac{j^m}{2\pi} \sum_{p=-\infty}^{\infty} \sum_{k'=0}^{\infty} \alpha_{(i),k'}^{(m)} \Lambda_{k'}^{(m)}(p) e^{jp\phi} \quad (4-9)$$

The real part of the line densities are shown in Fig.4, where we used a uniform scaling for the strength of the perturbation. For a half period of a synchrotron oscillation, 4 snapshots of the corresponding line density at the equally divided time period are shown in Fig.5, with only the first radial mode.

The following observations and deliberations are worth mentioning.

1. The initial condition of the perturbation  $\alpha_0$  determines the weighting of each eigenvalue. The way to find  $\alpha_0$  is by observing the line density generated by the initial perturbations, which are shown in Figs. 6-10 for first five radial modes separately. Note that the perturbation radial modes are shown on both side of (3-1), therefore the scaling is rather arbitrary. If the initial line density with perturbation is identified to be close to the waveform shown in Fig.7, which is due to the second radial mode, then the second eigenvalue will be dominant in the beam motion. An identification can also be made through the spectrum analysis. With the linearity of the integral equation, each mode will manifest itself with either the damping or growth rate, which is determined by the corresponding eigenvalue. Consider an unstable case. When the strength of a mode increases, the particle distribution in phase space will be changed. This change can be shown as a growth of the amplitude of the corresponding radial mode, as shown in Fig.3. Ideally, a growth of a radial mode is not coupled to other modes.

2. In Figs. 6-10, although the arbitrary scaling was mentioned, care has been taken to avoid the appearance of a negative part of the line density. In fact, when a mode continues to grow, inevitably an empty portion in phase space will be generated. Any further manifest by the mode creates negative line density in theory. In reality, this cannot happen. Instead, distortion will appear on the boundary of the empty zone. In Fig.11, we show line densities with a strong 5th radial mode along with the stationary distribution, which can be com-

1. Elliptic distribution ( Parabolic line density )

The stationary phase space density is

$$\psi_0(r) = \frac{3}{2\pi\hat{r}^2} \left(1 - \frac{r^2}{\hat{r}^2}\right)^{1/2} \quad (4-11)$$

The line density is,

$$\lambda_0(\phi) = \frac{3}{4\phi} \left(1 - \frac{\phi^2}{\hat{\phi}^2}\right) \quad (4-12)$$

The weight function can be calculated as

$$W(r) = \frac{-3}{2\pi\hat{r}^4} \left(1 - \frac{r^2}{\hat{r}^2}\right)^{-1/2} \quad (4-13)$$

Consider

$$\int_{-1}^1 P_k^{(\alpha,\beta)}(x) P_l^{(\alpha,\beta)}(x) (1-x)^\alpha (1+x)^\beta dx = h_k^{(\alpha,\beta)} \delta_{k,l}, \quad \alpha, \beta > -1 \quad (4-14)$$

where  $P_k^{(\alpha,\beta)}(x)$  is the Jacobi polynomial,

$$P_k^{(\alpha,\beta)}(x) = 2^{-k} \sum_{i=0}^k \binom{\alpha+k}{i} \binom{\beta+k}{k-i} (x-1)^{k-i} (x+1)^i \quad (4-15)$$

and with

$$h_k^{(\alpha,\beta)} = \frac{2^{\alpha+\beta+1}}{2k+\alpha+\beta+1} \frac{\Gamma(\alpha+k+1) \Gamma(\beta+k+1)}{k! + \Gamma(\alpha+\beta+k+1)} \quad (4-16)$$

Letting  $x = 1-2r^2/\hat{r}^2$ , then we get

$$\int_0^{\hat{r}} W(r) f_k(r) f_l(r) r dr = \int_{-1}^1 \frac{3}{2\pi\hat{r}^4} \frac{\hat{r}^2}{2\sqrt{2}} (x+1)^{-1/2} f_k(x) f_l(x) dx \quad (4-17)$$

Matching (4-17) with (4-14), we have  $\beta = -1/2$ , and also

$$f_k(x) = \left( \frac{4\sqrt{2}\pi\hat{r}^2}{3} \frac{(\alpha+2k+1/2) k! \Gamma(\alpha+k+1/2)}{2^{\alpha+1/2} \Gamma(\alpha+k+1) \Gamma(k+1/2)} \right)^{1/2} (1-x)^{\alpha/2} P_k^{(\alpha,-1/2)}(x) \quad (4-18)$$

Letting  $\alpha = m$ , we have,

$$f_k(r) = \left( \frac{4\pi(m+2k+1/2) k! \Gamma(m+k+1/2)}{3(m+k)! \Gamma(k+1/2)} \right)^{1/2} \hat{r} \left(\frac{r}{\hat{r}}\right)^m P_k^{(m,-1/2)}\left(1 - \frac{2r^2}{\hat{r}^2}\right) \quad (4-19)$$

In this and following examples, we use expansion of 7 orthogonal polynomials with  $p = \pm 10$ . The first 5 orthogonal polynomials are plotted in Fig.19. The radial modes with

We have

$$\int_0^{\hat{r}} W(r) f_k(r) f_l(r) r dr = \int_{-1}^1 \frac{15}{8\sqrt{2}\pi\hat{r}^2} (1+x)^{1/2} f_k(x) f_l(x) dx \quad (4-28)$$

Letting  $\alpha = m$  and  $\beta = 1/2$ , we have

$$f_k(r) = \left( \frac{4\pi (m+2k+3/2) k! \Gamma(m+k+3/2)}{15 \Gamma(m+k+1) \Gamma(k+3/2)} \right)^{1/2} \hat{r} \left( \frac{r}{\hat{r}} \right)^m P_k^{(m,1/2)} \left( 1 - \frac{2r^2}{\hat{r}^2} \right) \quad (4-29)$$

The orthogonal polynomials are plotted in Fig.25. The radial modes with inductive impedance are shown in Fig.26, and the corresponding line densities are shown in Fig.27.

## V. Solution Using Hankel Harmonic Samplings

The Sacherer integral equation (3-1) can also be solved by Hankel harmonic sampling of the radial modes at  $p$ , which represents frequencies, in an eigenvalue problem. We rewrite the equation (3-1) as,

$$\lambda R^{(m)}(r) = jm \omega_S \xi W(r) \sum_{p=-\infty}^{\infty} \frac{Z(p)}{p} J_m(pr) \Lambda^{(m)}(p) \quad (5-1)$$

Multiplying both side by  $J_m(qr)r$  and integrating over  $r$ , using (2-21), we get,

$$\lambda \Lambda^{(m)}(q) = jm \omega_S \xi \sum_{p=-\infty}^{\infty} \frac{Z(p)}{p} \int_0^{\infty} W(r) J_m(pr) J_m(qr) r dr \cdot \Lambda^{(m)}(p) \quad (5-2)$$

Running  $q$  from  $-\bar{p}$  to  $\bar{p}$ , then for  $p$  from  $-\bar{p}$  to  $\bar{p}$ , we have,

$$\lambda \begin{bmatrix} \Lambda^{(m)}(-\bar{p}) \\ \vdots \\ \Lambda^{(m)}(\bar{p}) \end{bmatrix} = jm \omega_S \xi \mathbf{K} \begin{bmatrix} \Lambda^{(m)}(-\bar{p}) \\ \vdots \\ \Lambda^{(m)}(\bar{p}) \end{bmatrix} = jm \omega_S \xi \begin{bmatrix} K_{-\bar{p},-\bar{p}}^{(m)} & \cdots & K_{\bar{p},-\bar{p}}^{(m)} \\ \vdots & \ddots & \vdots \\ K_{-\bar{p},\bar{p}}^{(m)} & \cdots & K_{\bar{p},\bar{p}}^{(m)} \end{bmatrix} \begin{bmatrix} \Lambda^{(m)}(-\bar{p}) \\ \vdots \\ \Lambda^{(m)}(\bar{p}) \end{bmatrix} \quad (5-3)$$

where

$$K_{p,q}^{(m)} = \frac{Z(p)}{p} \int_0^{\infty} W(r) J_m(pr) J_m(qr) r dr \quad (5-4)$$

The equation (5-3) is also an eigenvalue problem.

To find the relation between the two approaches, we have the following equation according to (3-5),

set of eigenvalues. Even though the dimensions of the two matrices are different, by an inspection it can be found that the computing load is the same, i.e. both need the Hankel spectra for orthogonal polynomials shown in (3-4).

2. Using the harmonic sampling approach, the matrix  $\mathbf{K}$  can be calculated by the Bessel functions as shown in (5-4). The equation (3-6) shows that the Bessel function is equivalent to an expansion of the orthogonal polynomials with an infinite order. Meanwhile in the orthogonal polynomial approach,  $k$  has to be truncated. If the convergence in the orthogonal polynomial expansion is guaranteed and it is fast, then the difference between the two approaches will not be important. Otherwise, the Bessel function calculation can be used to verify the accuracy of the orthogonal polynomial approach. In Fig.28, the Bessel function  $J_1(pr)$  with  $p = 1, 2, 3, 4, 5$  are shown, compared with the dotted lines for the orthogonal polynomial approximation using (3-6), where the Gaussian distribution and up to 5th order orthogonal polynomials are used. It can be observed that to let the approximation acceptable, in this case, for the harmonic number larger than 5 a higher order orthogonal polynomial expansion is needed.

3. In the orthogonal polynomial approach, sometimes the harmonic number can be extended to be very large by an analytical expression of the component in the matrix  $\mathbf{M}$ . Consider an inductive impedance, and assume that the perturbation line density of each orthogonal polynomial is known. We may write

$$\begin{aligned} M_{k,l}^{(m)} &= \sum_{p=-\infty}^{\infty} \Lambda_k^{(m)}(p) \Lambda_l^{(m)}(p) = \sum_{p=-\infty}^{\infty} \int_{-\infty}^{\infty} \lambda_k^{(m)}(\phi) e^{-jp\phi} d\phi \int_{-\infty}^{\infty} \lambda_l^{(m)}(\phi') e^{-jp\phi'} d\phi' \\ &= 2\pi \int_{-\infty}^{\infty} \lambda_k^{(m)}(\phi) \lambda_l^{(m)}(-\phi) d\phi \end{aligned} \quad (5-10)$$

The last step in (5-10) requires that the harmonic number  $p$  be very large, therefore this expression includes very high harmonics. Whereas in the harmonic sampling approach, the number of the orthogonal polynomials is infinite, but the harmonic number is limited. This condition for using (5-10) is crucial and very restricted, therefore the usage of this method is limited.

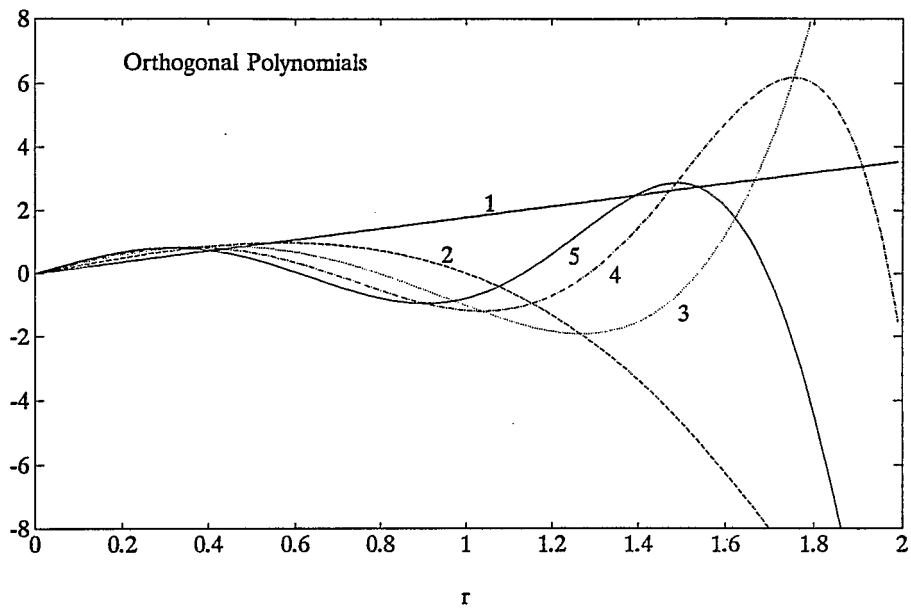


Fig.1. Orthogonal Polynomials for Gaussian Distribution.

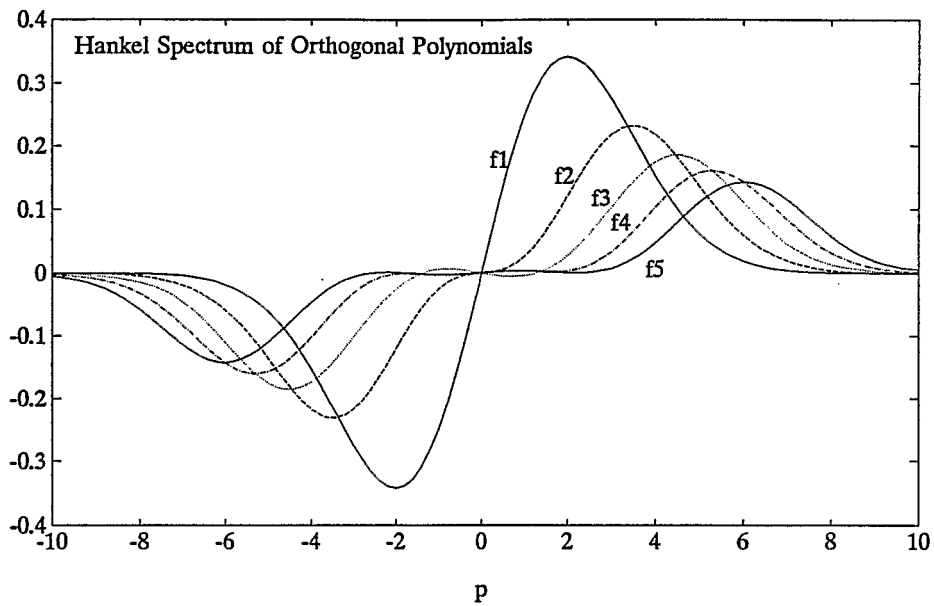


Fig.2. Hankel Spectra of Orthogonal Polynomials for Gaussian Distribution.

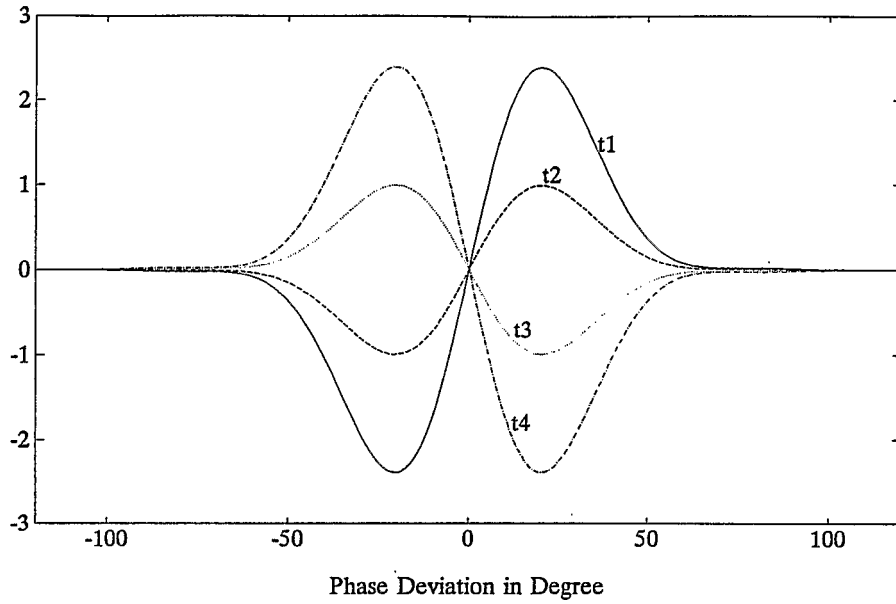


Fig.5. Snapshot of Line Density of 1st Radial Mode for Gaussian Distribution.

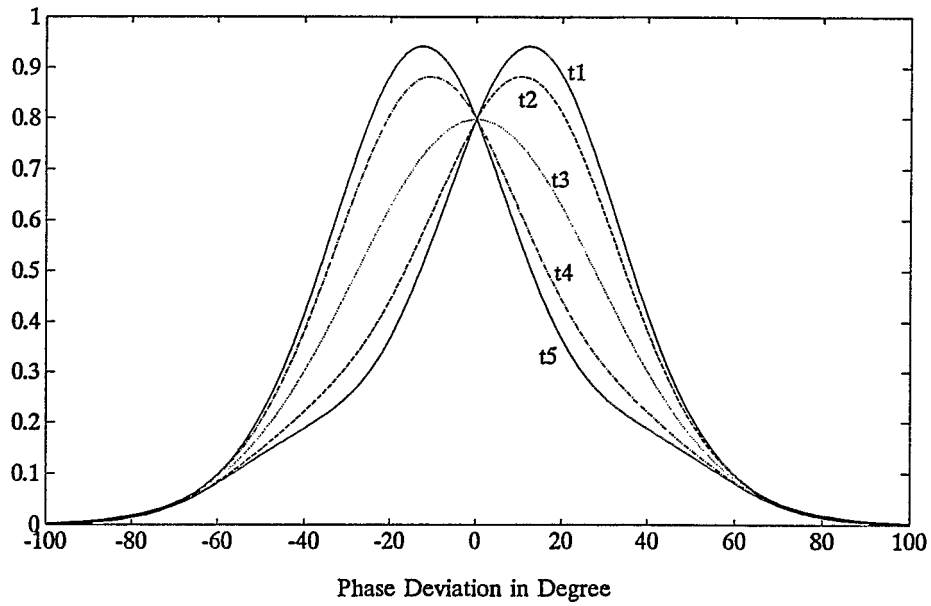


Fig.6. Line Density of Stationary Distribution and 1st Radial Mode, Gaussian.

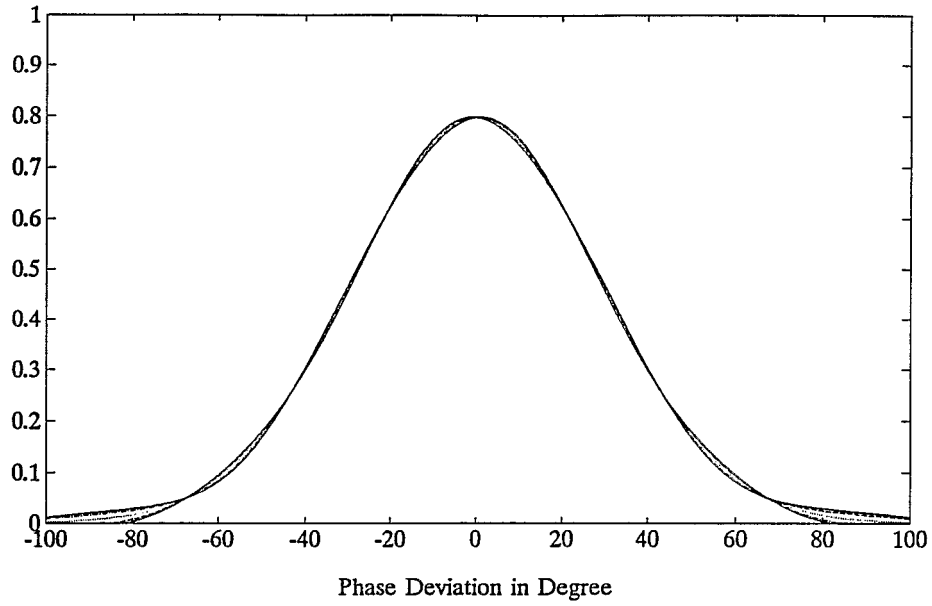


Fig.9. Line Density of Stationary Distribution and 4th Radial Mode, Gaussian.

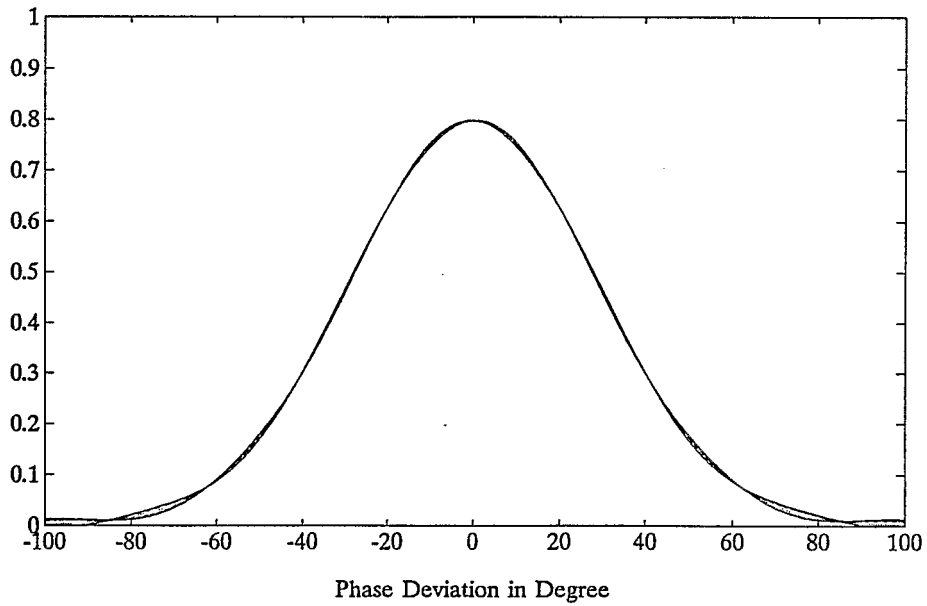


Fig.10. Line Density of Stationary Distribution and 5th Radial Mode, Gaussian.

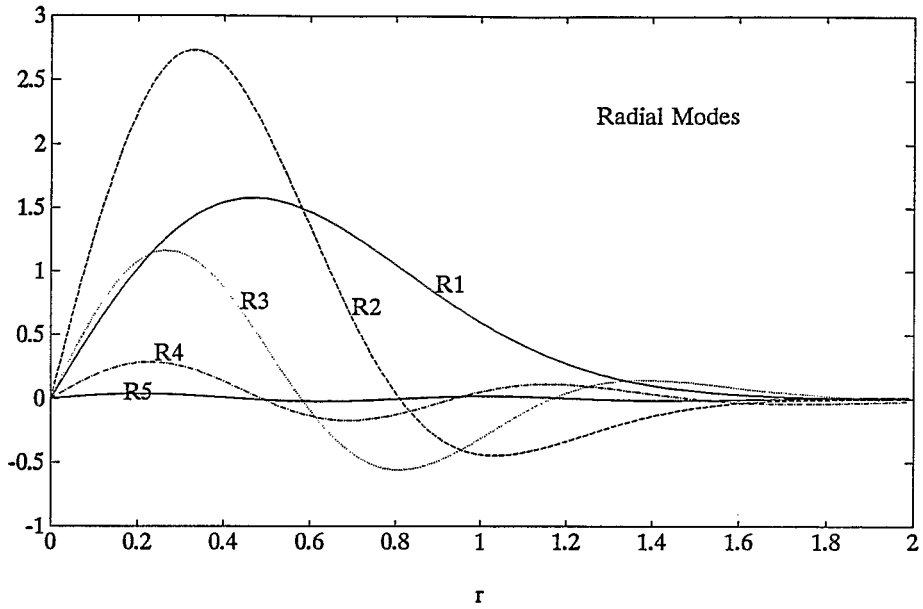


Fig.13. Radial Modes with a Narrow Band Cavity, Gaussian.

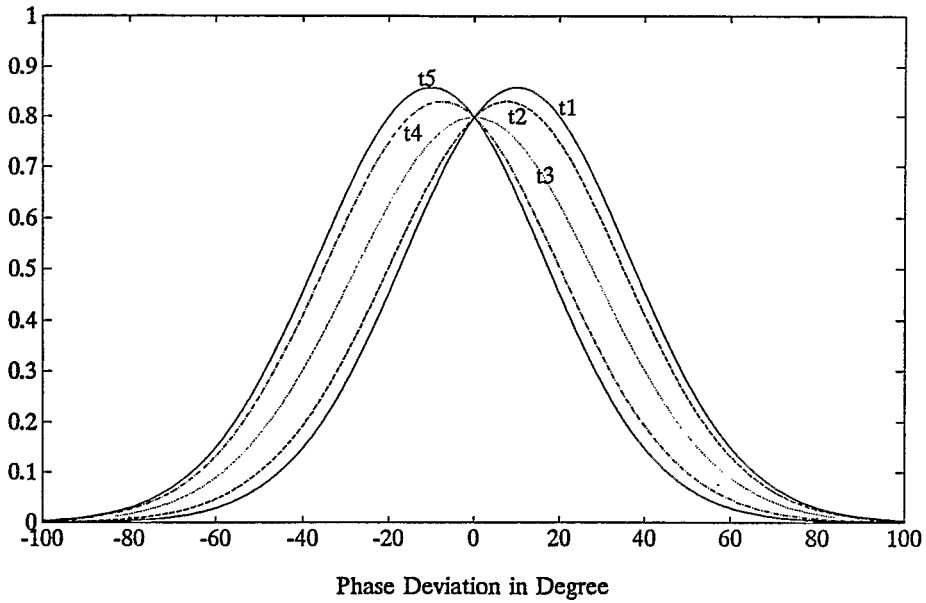


Fig.14. Line Density of Stationary Distribution and 1st Radial Mode.

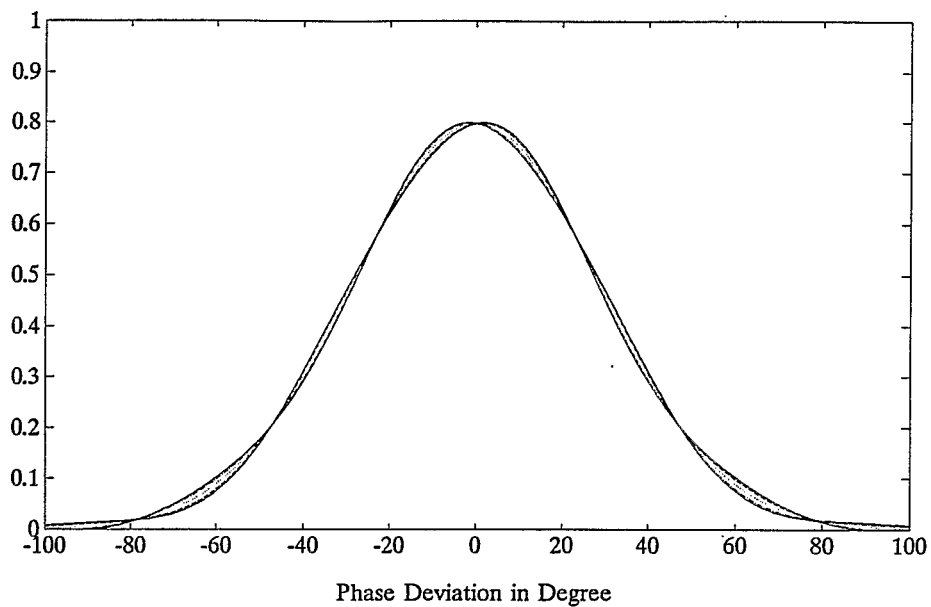


Fig.17. Line Density of Stationary Distribution and 4th Radial Mode.

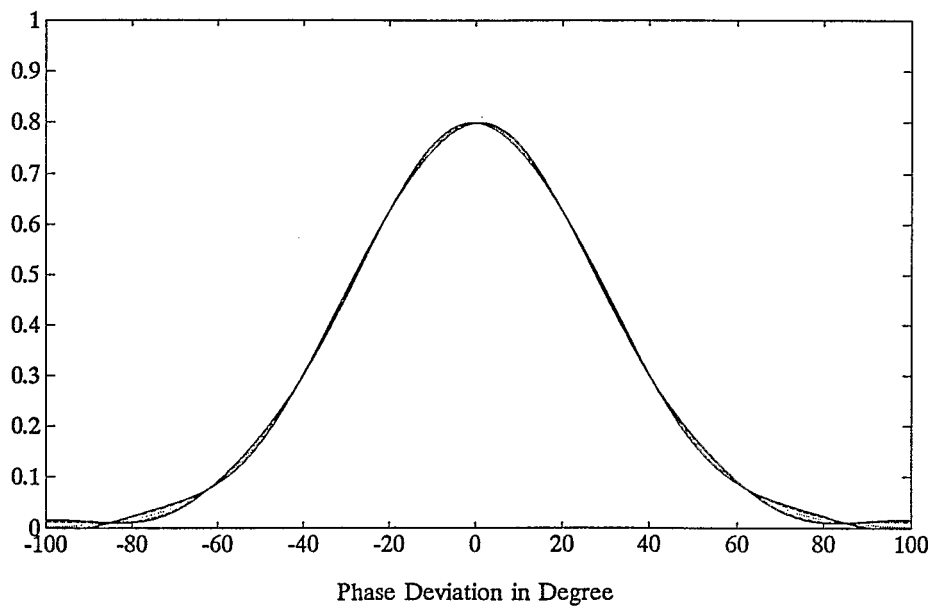


Fig.18. Line Density of Stationary Distribution and 5th Radial Mode.

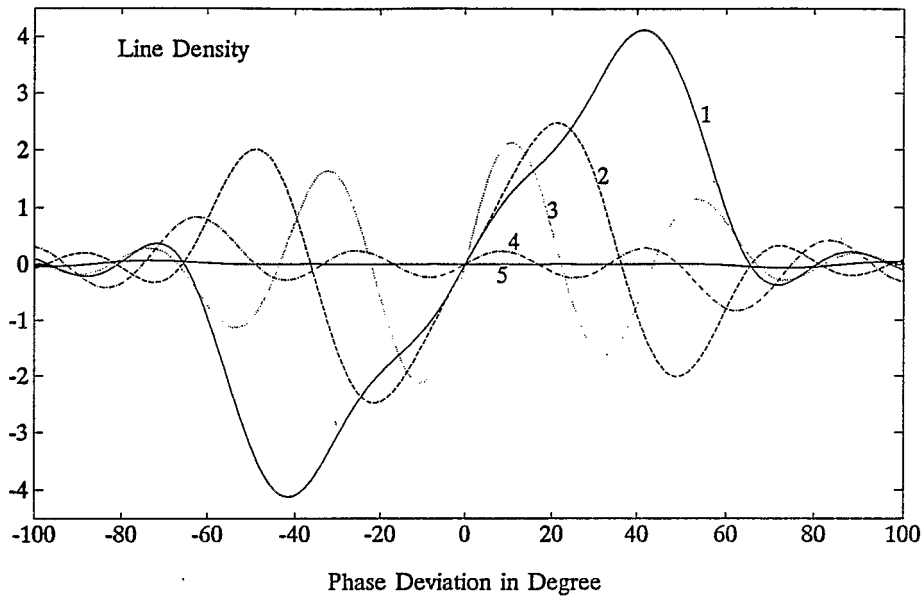


Fig.21. Line Density of Elliptic Distribution.

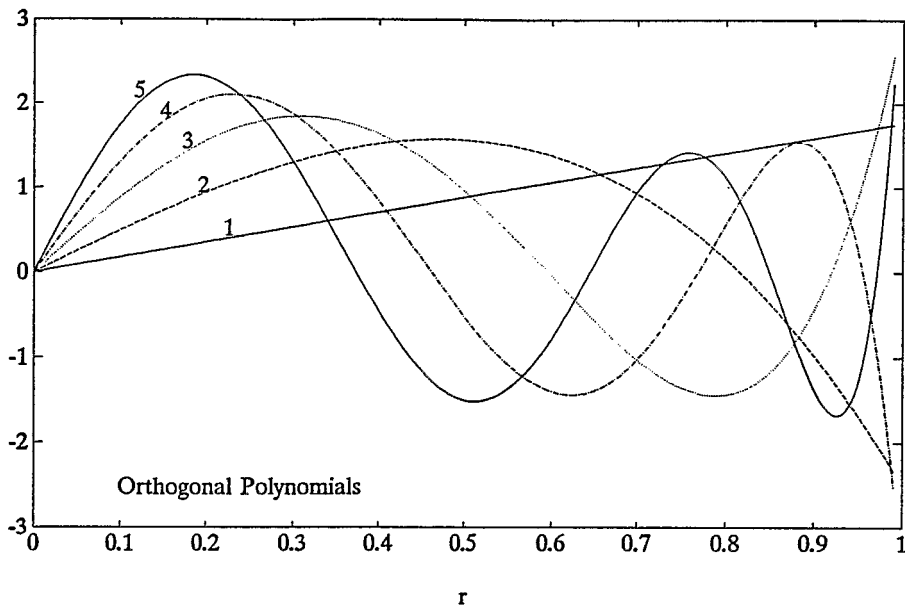


Fig.22. Orthogonal Polynomials of Parabolic Distribution.

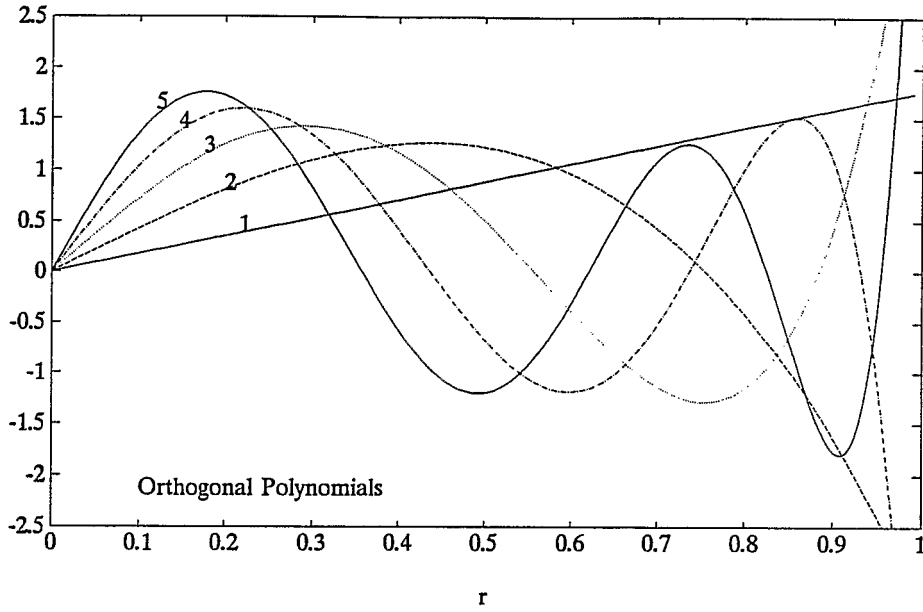


Fig.25. Orthogonal Polynomials of Elliptic Weight Function Distribution.

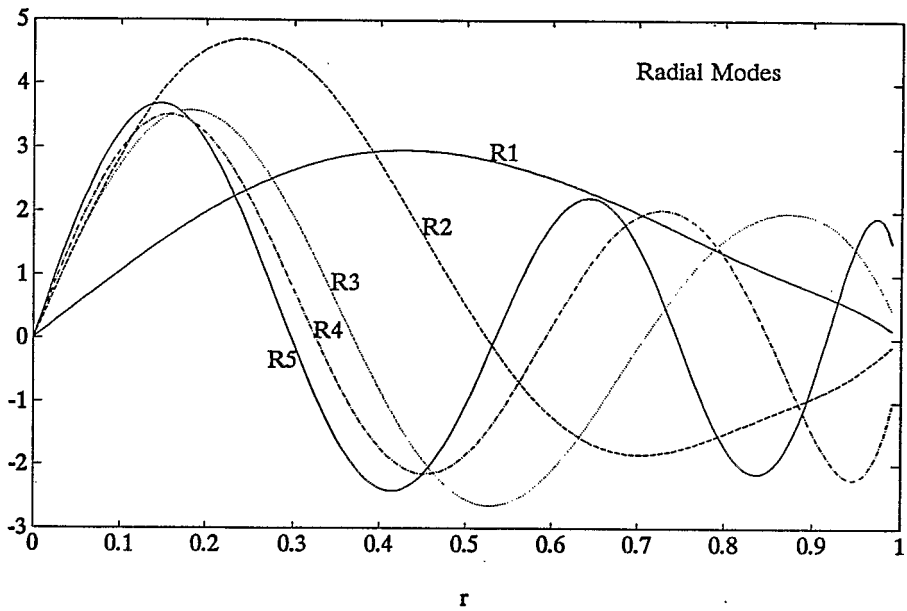


Fig.26. Radial Modes of Elliptic Weight Function Distribution.